Supplementary Information

Observation of binding of carbon dioxide to nitro-decorated metal-organic frameworks

Thien D. Duong,[1] Sergey A. Sapchenko,[1] Ivan da Silva,[2] Harry G.W. Godfrey,[1] Yongqiang Cheng,[3] Luke L. Daemen[3], Pascal Manuel,[2] Mark D. Forgley,[4] Gianfelice Cinque,[4] Anibal J. Ramirez-Cuesta,[3] Sihai Yang[1]* and Martin Schröder[1]*

1. School of Chemistry, University of Manchester, Manchester, M13 9PL, UK.
2. ISIS Facility, STFC Rutherford Appleton Laboratory, Chilton, Oxfordshire, OX11 0QX, UK.
3. Oak Ridge National Laboratory, Oak Ridge, TN 37831, USA.
4. Diamond Light Source, Harwell Science and Innovation Campus, Oxfordshire, UK.

1. Synthesis and characterisation

The synthesis and characterisation of MOF materials was undertaken according to the literature.[1]

2. Gas adsorption at 273 K

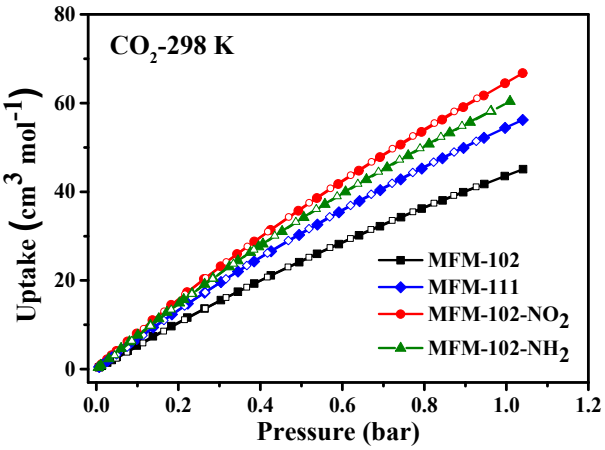

Figure S1. Experimental sorption isotherms for CO_2 in the MFM-102 series of materials. Adsorption (filled symbols) and desorption (empty symbols).

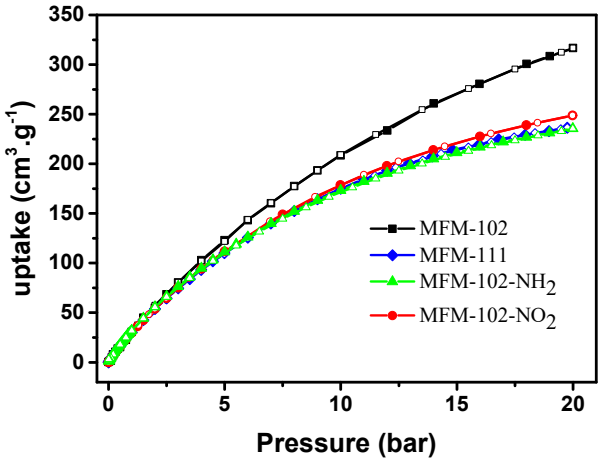

Figure S2. Experimental sorption isotherms for CH_4 in the MFM-102 series of materials up to 20 bar at 273 K. Adsorption (filled symbols) and desorption (empty symbols).

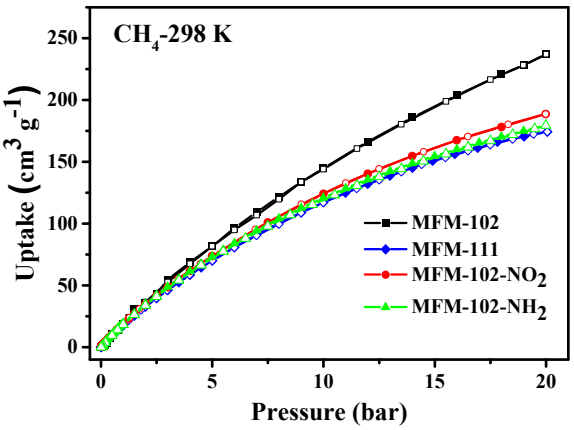

Figure S3. Experimental sorption isotherms for CH_4 in the MFM-102 series of materials up to 20 bar at 273 K. Adsorption (filled symbols) and desorption (empty symbols).

3. Heats of adsorption

The presence of a relatively strong interaction between gas molecules and the frameworks was revealed by analysis of the coverage-dependent isosteric heats of adsorption (*Qst*). The virial-type expression comprising the temperature-independent parameters a_i and b_j was employed to calculate the Q_{st} of all the gases by measuring isotherms at 273 K and 298 K. In each case, the data were fitted using the equation below:

$$ln(P) = ln(N) + \left(\frac{1}{T}\right)\sum_{i=0}^{m} a_i N^i + \sum_{j=0}^{n} b_j N^j$$

where the pressure is expressed in bar, N is the amount of adsorbed in mmol g^{-1}, T is the temperature in K, a_i and b_j are Virial coefficients, and m and n represent the number of parameters required to describe the isotherms (in this case, m and n were fixed at 5 and 4, respectively). The values of Viral coefficients a_0 – a_m were then used to estimate the value of Q_{st} using the following expression with the universal gas constant R:

$$Q_{st} = -R\sum_{i=0}^{m} a_i N^i$$

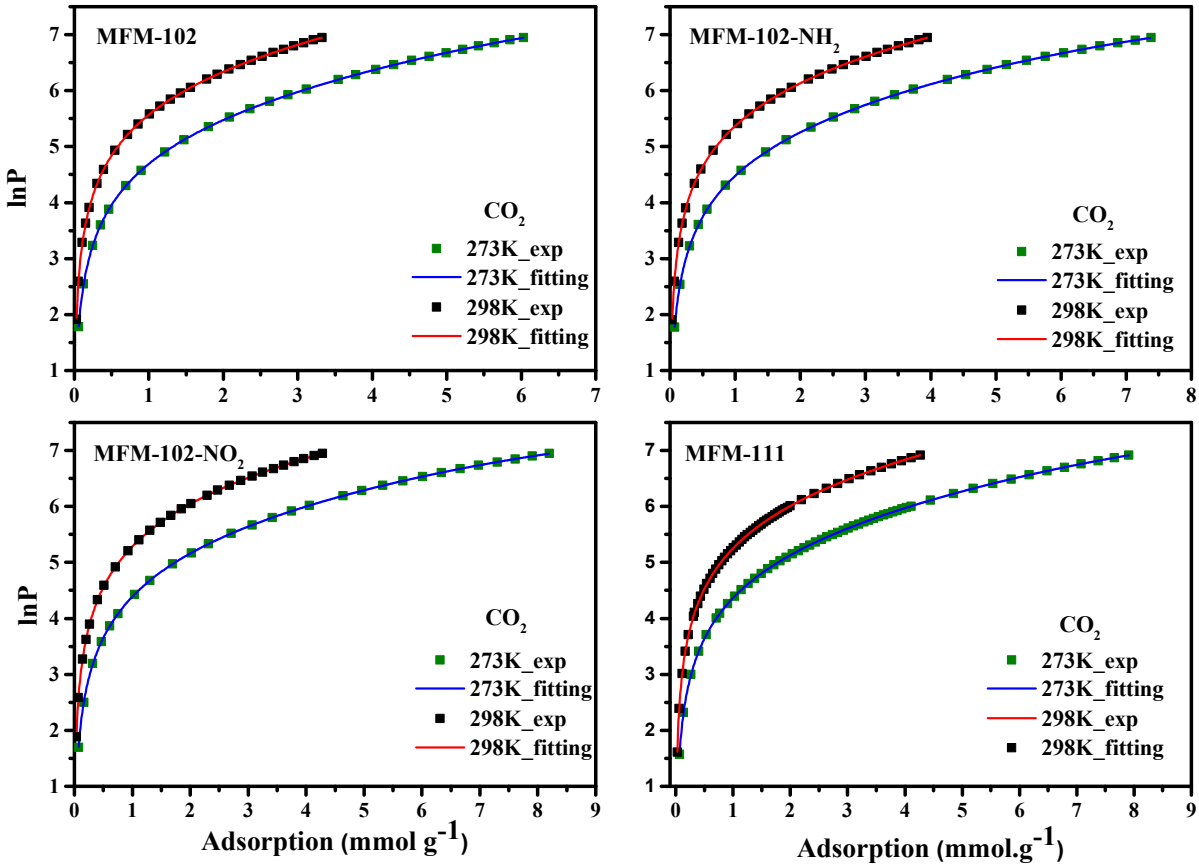

Figure S4. Virial fitting for CO_2 adsorption in the MFM-102 series of MOFs at 273 and 298 K.

4. Determination of selectivity for gas mixtures in the MFM-102-NO_2 series.

In order to perform IAST calculations, the single-component isotherm was fitted using the dual-site Langmuir Freundlich (DSLF) adsorption model to correlate the pure-component equilibrium data and further predict the adsorption of mixtures.

$$q = q_{m1}.\frac{b_1.P^{1/n_1}}{1 + b_1.P^{1/n_1}} + q_{m2}.\frac{b_2.P^{1/n_2}}{1 + b_2.P^{1/n_2}}$$

where P is the pressure of the bulk gas at equilibrium with the adsorbed phase (kPa), q is the adsorbed amount per mass of adsorbent (mol kg^{-1}), qm_1 and qm_2 are the saturation capacities of sites 1 and 2 (mol kg^{-1}), b_1 and b_2 are the affinity coefficients of sites 1 and 2 ($1/kPa$), and n_1 and n_2 represent the deviations from an ideal homogeneous surface. If the fitting does not converge, the single site Langmuir Freundlich can be used by fixing the value of q_{m2} to 0.

The selectivity of preferential adsorption of component 1 over component 2 in a mixture containing 1 and 2 can be formally defined as:

$$S_{1,2} = \frac{x_1/y_1}{x_2/y_2}$$

Where x_1 and x_2 are the molar ratios of the adsorbed gases and y_1 and y_2 are the molar fractions of the gas phases. Based on the above model parameters of pure gas adsorption from DSLF model, we used the IAST model[2] to predict the multi-component adsorption, in another way, calculating the values of x_1 and x_2.

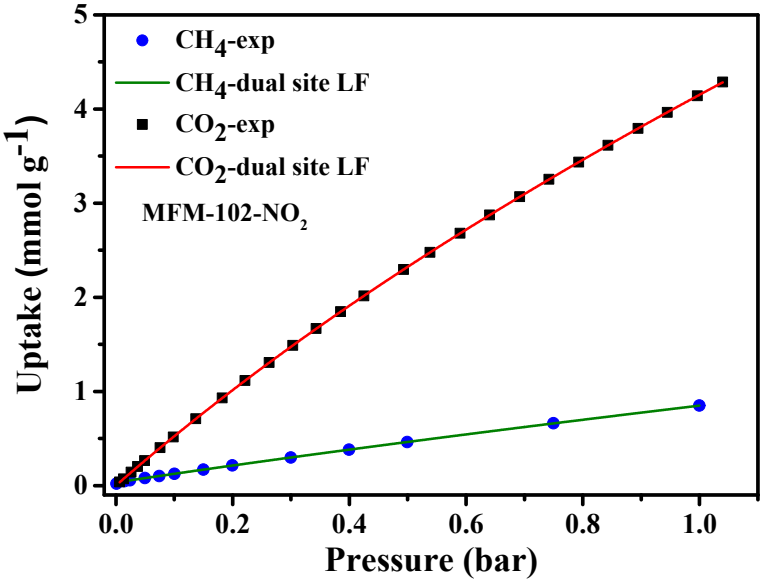

Figure S5. Single/Dual-site Langmuir Freundlich fitting (continuous line) and experimental data (solid points) for CH_4 and CO_2 in MFM-102-NO_2.

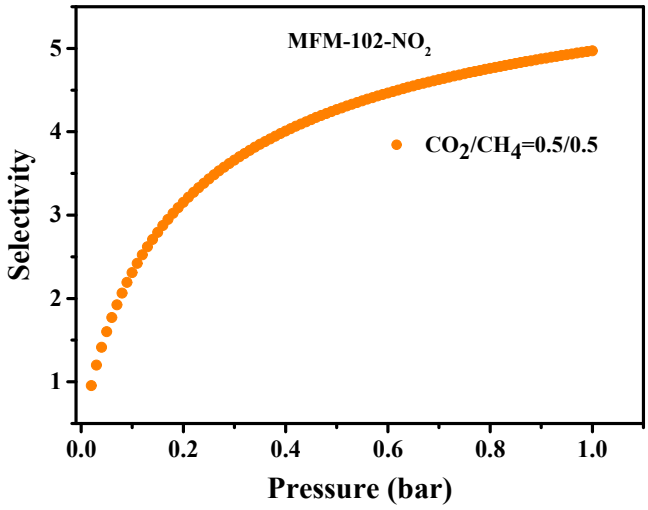

Figure S6. IAST selectivity plot for a CO_2/CH_4 (50:50) gas mixture in MFM-102-NO_2 at 298 K.

5. Synchrotron FTIR microspectroscopy of CO_2-loaded MFM-102-NO_2

Table S1. Frequency of IR active vibrational modes in gaseous and adsorbed CO_2 in MFM-102-NO_2.

CO_2 vibrational mode	Frequency in gaseous CO_2 (cm^{-1})	Frequency in adsorbed CO_2 (cm^{-1})
ν_2	667	660
ν_3	2349	2341
$2\nu_2 + \nu_3$	3612	3600
$\nu_1 + \nu_3$	3714	3700

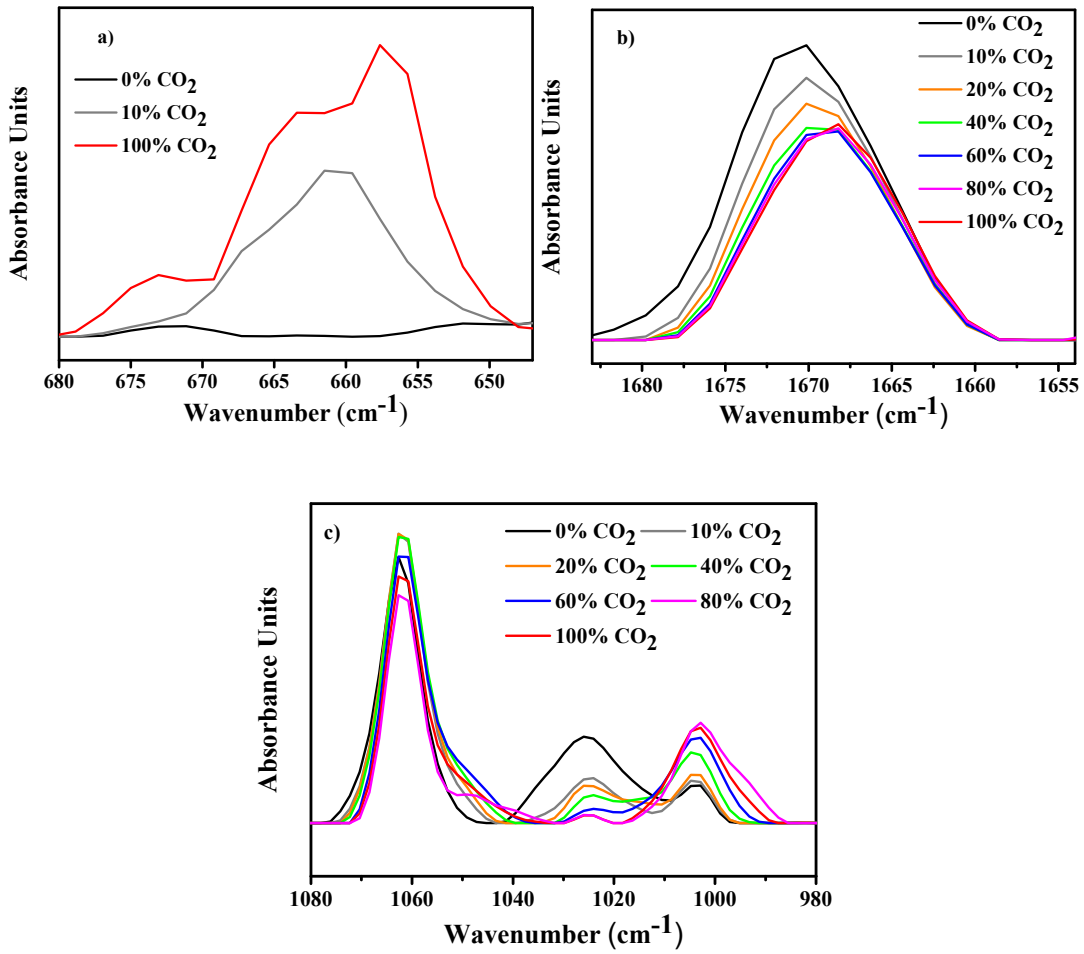

Figure S7. FTIR microspectroscopy of CO_2-loaded MFM-102-NO_2. a) The ν_2 bending mode grows and splits into two peaks, indicating the removal of the degeneracy while CO_2 molecules bind to open Cu(II) sites. b) The carboxylate C═O stretching vibration at 1670 cm^{-1} red shifts by 2 cm^{-1}. c) The in-plane phenyl ring deformation and C-H out of plane bending at 1025 cm^{-1} nearly disappears at 100% CO_2 loading, while the bend at 1005 cm^{-1} slowly increases in intensity with increasing CO_2 loading.

6. Inelastic neutron scattering and DFT calculations

INS spectra were recorded on the VISION spectrometer at the Spallation Neutron Source, Oak Ridge National Laboratory (USA). VISION is an indirect geometry crystal analyser instrument that provides a wide dynamic range with high resolution. A sample of desolvated MFM-102-NO_2 was loaded into an 11 mm cylindrical vanadium sample container, sealed with an indium vacuum seal and connected to a gas handling system. The sample was degassed at 10^{-7} mbar and 373 K for 2 days prior to the experiment to remove any remaining trace guest molecules. Gas loading was performed by a volumetric method at 293 K in order to ensure that the adsorbent was available in the gas phase and to ensure sufficient mobility within the crystalline structure of MFM-102-NO_2. The sample was then slowly cooled to 10 K to ensure the guest molecule of interest was completely adsorbed with no condensation in the cell. Sufficient time was allowed to achieve thermal equilibrium before inelastic neutron spectra were collected to allow for full thermal equilibrium before data collection.

Vibrational frequencies and polarization vectors were calculated using CP2K (http://www.cp2k.org),[3] based on the mixed Gaussian and plane-wave scheme[4] and the Quickstep module.[5] The calculation used molecularly optimized Double-Zeta-Valence plus Polarization (DZVP) basis set,[6] Goedecker-Teter-Hutter pseudopotentials,[7] and the Perdew-Burke-Ernzerhof (PBE) exchange correlation functional.[8] The plane-wave energy cut-off was 400 Ry. A DFT-D2 level correction for dispersion interactions, as implemented by Grimme et al,[9] was applied, with a cut-off distance of 24 Å. The calculation was performed on Gamma point only, with no symmetry constraint. Structural optimization was performed using the Broyden-Fletcher-Goldfarb-Shannon (BFGS) optimizer, until the maximum force is below 0.00045 Ry/Bohr (0.011 eV/Å). Finite displacement method was used for the phonon calculation, with incremental displacement of 0.01 Bohr (0.0053 Å). The INS spectrum was then simulated using the OClimax software.[10,11]

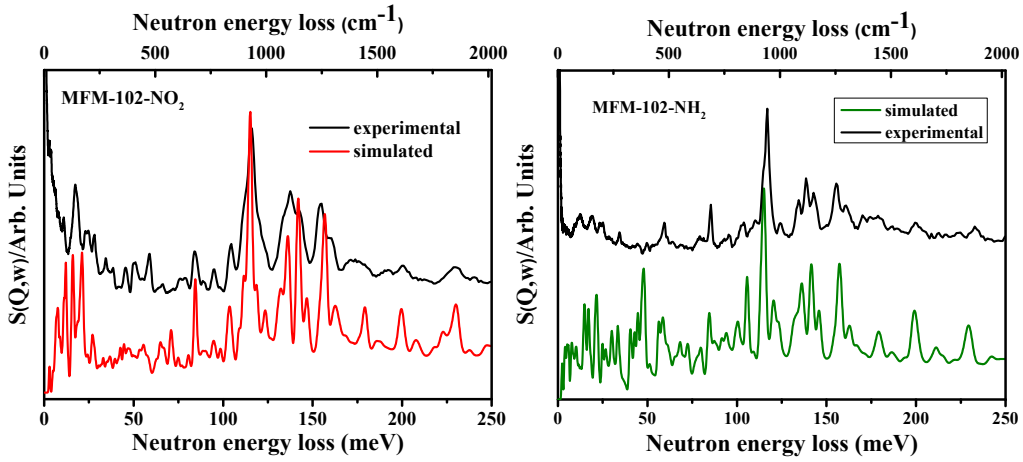

Figure S8. INS spectra of activated MFM-102-NO_2 (left) and MFM-102-NH_2 (right) and the corresponding simulated spectra from DFT calculations.

7. Neutron powder diffraction

NPD experiments were conducted at WISH, a long wavelength powder and single crystal diffractometer at the ISIS facility (DOI: 10.5286/ISIS.E.82420531). Acetone-exchanged MFM-102-NO_2 was loaded into a 6 mm diameter vanadium sample can and outgassed at 1 x 10^{-7} mbar and 110 ^{o}C for 1 day. The sample stick was then placed into a liquid He cryostat and cooled to 7K for data collection of the activated framework. CO_2 gas was introduced sequentially into the framework by warming the sample to 290 K. The gas was dosed volumetrically from a calibrated volume. The gas containing sample was then gradually cooled to 7 K over 2 h to ensure good diffusion of adsorbed gases within the crystalline structure of MFM-102-NO_2 and to minimise the presence of "free gas" or condensation inside the cell. The sample was kept at 7 K for sufficient time to achieve thermal equilibrium before collecting data.

The locations of adsorbed CO_2 molecules within MFM-102-NO_2 were determined as a function of gas loading by sequential Fourier difference map analysis followed by Rietveld refinement using the Topas software package. Analysis of the Fourier map of the outgassed data indicated no residual nuclear density in the voids. The structure from the single crystal X-ray diffraction experiment was used as a starting point for the framework model which was geometrically restrained and refined against the NPD data. The atom coordinates of the framework were subsequently fixed before models for guest molecules were developed. All binding sites were checked carefully for their unambiguous presence in the final structural model; *i.e.*, a parallel refinement without each of the binding sites was carried out to confirm the presence of each site by comparing R factors and residual peaks. The final refinements on all the parameters including fractional coordinates, thermal parameters, occupancies for both host lattice and adsorbed CO_2 molecules, and background/profile coefficients yielded very good agreement factors. No restriction of the molecule position was used in the refinement. The total occupancies of CO_2 molecules obtained from the refinement are also in good agreement with the experimental values for the CO_2 loading.

Table S2. Refinement parameters from NPD data.

	Activated MOF	**CO_2-loaded MOF**
R_{exp}/%	0.26	0.26
R_{wp}/%	1.45	1.25
R_p/%	1.24	1.13
GoF	5.43	4.72
CCDC Deposit	1857873	1860478

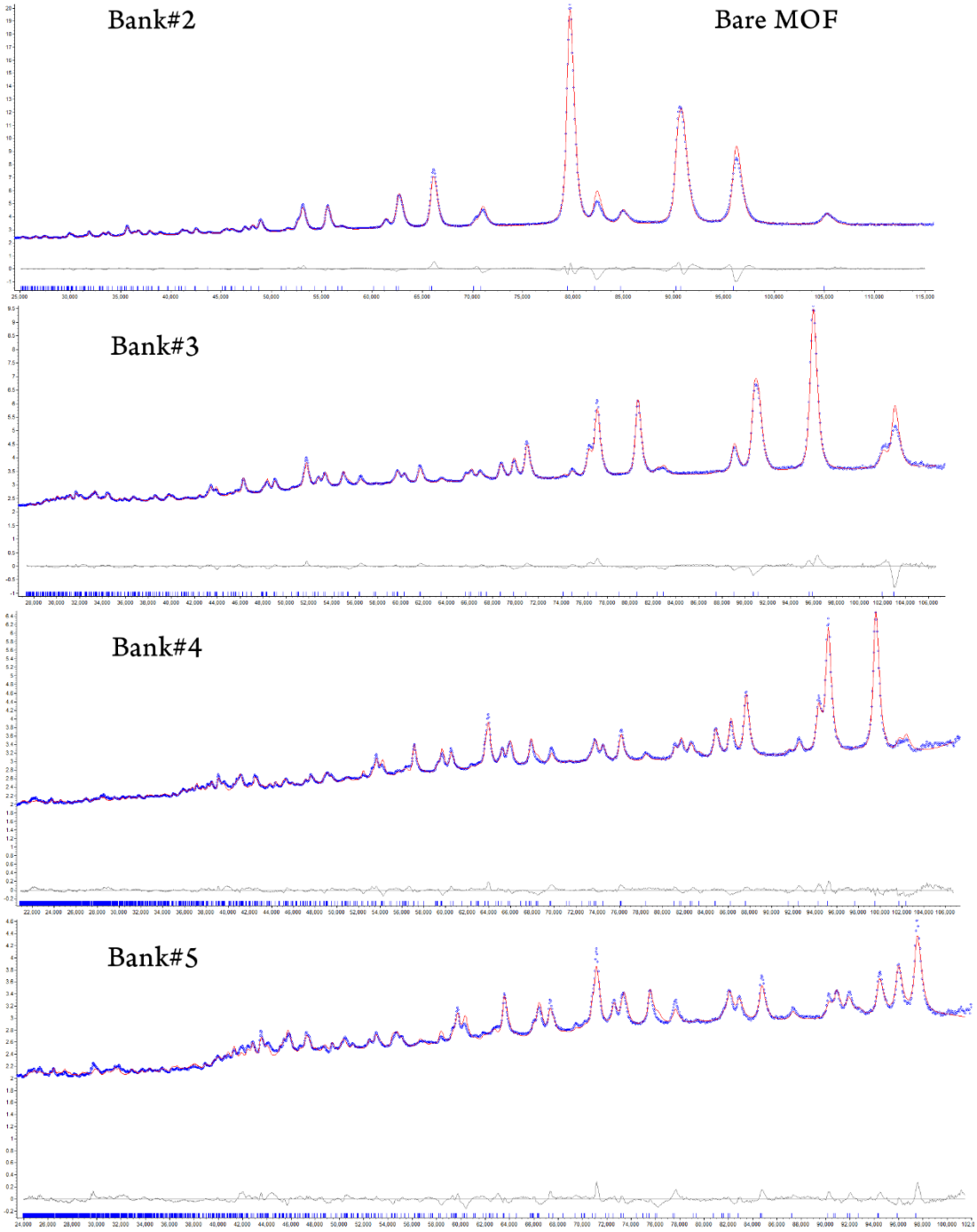

Figure S9. Observed (blue), calculated (red) and difference (grey) profiles of Rietveld refinements of neutron powder diffraction data (detector banks 2-5) for activated MFM-102-NO_2.

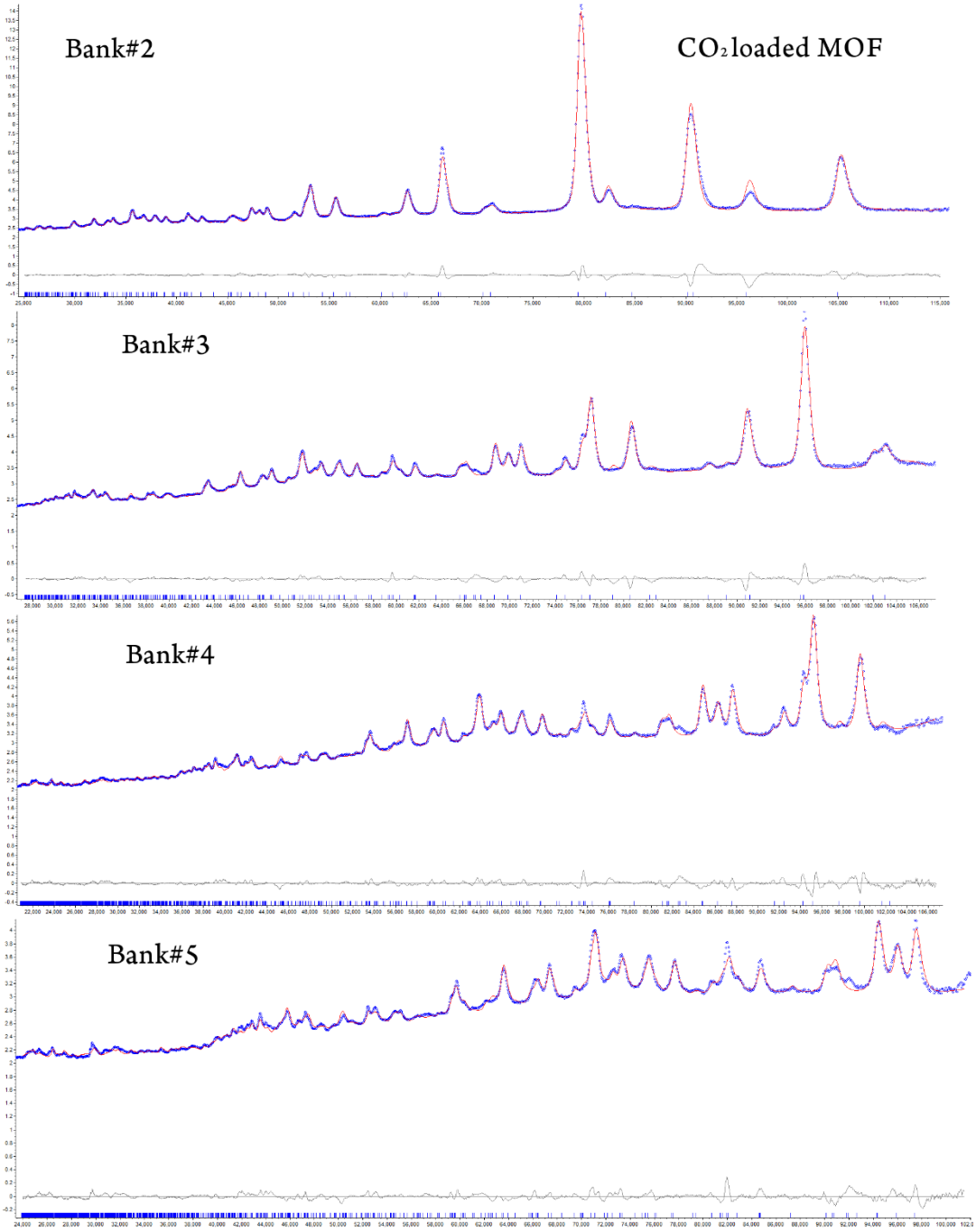

Figure S10. Observed (blue), calculated (red) and difference (grey) profiles of Rietveld refinements of neutron powder diffraction data (detector banks 2-5) for MFM-102-NO_2 loaded with CO_2.

Reference:

1. T. D. Duong, S. A. Sapchenko, I. da Silva, H. G. W. Godfrey, Y. Cheng, L. L. Daemen, P. Manuel, A. J. Ramirez-Cuesta, S. Yang and M. Schröder, *J. Am. Chem. Soc.*, 2018, **140**, 16006-16009.
2. A. L. Myers and J. M. Prausnitz, *AIChE*, 1965, **11**, 121-127.
3. J. Hutter, M. Iannuzzi, F. Schiffmann and J. VandeVondele, *WIREs Comput. Mol. Sci.*, 2014, **4**, 15-25.
4. B. G. Lippert, J. H. Parrinello and Michele, *Mol. Phys.*, 1997, **92**, 477-488.
5. J. VandeVondele, M. Krack, F. Mohamed, M. Parrinello, T. Chassaing and J. Hutter, *Comput. Phys. Commun.*, 2005, **167**, 103-128.
6. J. VandeVondele and J. Hutter, *J. Chem. Phys.*, 2007, **127**, 114105.
7. S. Goedecker, M. Teter and J. Hutter, *Phys. Rev. B*, 1996, **54**, 1703-1710.
8. J. P. Perdew, K. Burke and M. Ernzerhof, *Phys. Rev. Lett.*, 1996, **77**, 3865-3868.
9. S. Grimme, *J. Comput. Chem.*, 2006, **27**, 1787-1799.
10. A. J. Ramirez-Cuesta, *Comput. Phys. Commun.*, 2004, **157**, 226-238.
11. https://sites.google.com/site/ornliceman/download.

Author contributions

TDD, SAS: synthesis and preparation of materials for measurements and gas isotherms

IdS, PM, SAS, TDD: *in situ* neutron data collection and structural analyses

HGWG, YC, LLD AJR-C: inelastic neutron scattering experiments

MDF, GC: micro-infrared spectroscopy

SY, MS: design, development and supervision of the project